Prediction of Ethene + Oct-1-ene Copolymerization Ideal Conditions Using Artificial Neuron Networks

ARTICLE *in* JOURNAL OF CHEMICAL & ENGINEERING DATA · SEPTEMBER 2010

Impact Factor: 2.04 · DOI: 10.1021/je1001973

5 AUTHORS, INCLUDING:

Juan Angel Ferreiro-Lage
Indra
14 PUBLICATIONS **80** CITATIONS
SEE PROFILE

J.F Galvez
University of Vigo
22 PUBLICATIONS **104** CITATIONS
SEE PROFILE

Juan C. Mejuto
University of Vigo
376 PUBLICATIONS **2,673** CITATIONS
SEE PROFILE

Prediction of Ethene + Oct-1-ene Copolymerization Ideal Conditions Using Artificial Neuron Networks

G. Astray,[†] P. V. Caderno,[‡] J. A. Ferreiro-Lage,[†] J. F. Galvez,[‡] and J. C. Mejuto*,[†]

Department of Physical Chemistry, Faculty of Sciences, University of Vigo at Ourense, 32004, Ourense, Spain, and Department of Informatics, ESEI, University of Vigo at Ourense, 32004, Ourense, Spain

The most influential parameters on polymerization of ethene + oct-1-ene using a metallocene catalyst system are temperature, ethene pressure, and the amount of hydrogen used for polymerization. An implemented artificial neural network (ANN) is a supervised back-propagation model with different architectures. An ANN for determining the conditions in the copolymerization of ethene + oct-1-ene using a metallocene catalyst system to produce a copolymer with specific chains has been implemented. It has been shown that the proper functioning of the ANN is implemented with satisfactory *R* values. Therefore, it is concluded that the ANN developed is an effective tool to determine the conditions of copolymerization of ethene and oct-1-ene.

Introduction

The ethene + oct-1-ene copolymer is a polymer that can be synthesized in a wide range by controlling different parameters. A metallocene catalyst system is the most efficient process to produce this polymer (see Scheme 1), and they are operative in all existing industrial plants that are presently used for polyolefin manufacturing and have the potential to revolutionize the technology for the production of these polymers.[1−5] They show extreme promise in the production of α-olefins (small plastic building blocks).

Polyolefins are among the most important modern commodity polymers. A polyolefin elastomer (or POE) is a relatively new class of polymers that emerged with recent advances in the metallocene polymerization catalyst. It represents one of the fastest growing synthetic polymers. POE's can be substituted for a number of generic polymers including ethene propene rubbers (EPR or EPDM), ethene vinyl acetate (EVA), styrene-block copolymers (SBCs), and polyvinyl chloride (PVC).

POEs are compatible with most olefinic materials, are an excellent impact modifier for plastics, and offer unique performance capabilities for compounded products. Polyethene and polypropene are today the most major tonnage plastic materials worldwide. These two resins accounted for over 40 % of all plastic sales in 1988. The industrial capacity for the production of polyethene and polypropene in 1990 was ∼45 million tons.[6,7]

The main question about industrial synthesis of these polymers is finding the optimal conditions to obtain a copolymer with the desired hydrocarbon chain.[1] This problem would normally be solved by means of trial-and-error experiments, which entail a great loss of money, resources, and time. An alternative system could be the performance of an analysis of the parameters that control the process. Therefore, it is our intention to demonstrate through this study the suitability of using artificial neural networks (ANNs) to determine these copolymerization parameters.

Scheme 1

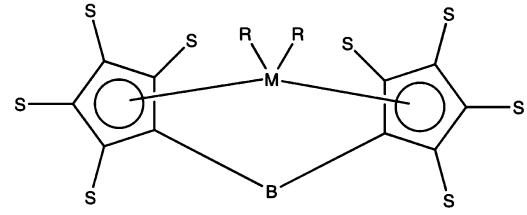

M: Transition metal
R: Hydrocarbyl, Alkylidene, Halogen Radicals
B: Alkylene, Alkyl radicals, Heteroatom groups

ANNs are a complete statistical tool for data analysis.[8] The ANN origin dates back to the middle of the last century when an interdisciplinary group of biologists, psychologists, and engineers with an interest in understanding the functioning of the human brain was created.[9] The ANNs try to reproduce artificially the human ability of taking decisions simulating human brain's basic unit, the neuron, and the interconnections between neurons that allow them to work together and save the experience information.[10] ANNs, hence, are black-box models with a high capability to simulate dynamic nonlinear systems. The original artificial neuron is the threshold logic unit proposed in the first part of the last century,[11] but in recent years, ANNs have been extended successfully to very different fields, from hydrology to finances.[12] Neural networks have also been used in aerobiological studies to achieve predicting models to improve the daily pollen concentration forecast.[13,14]

An ANN is a mathematical tool which tries to represent low-level intelligence in natural organisms, and it is a flexible structure, capable of making a nonlinear mapping between input and output spaces.[15] We could define an ANN as a system for the treatment of information whose basic processing unit is inspired in the main human brain cell. ANNs were originally an abstract simulation of the biological brain systems, composed of an assembly of units called "neurons" (or "nodes") connected between them. An artificial neuron, also called semilinear unit,

* Corresponding author. Tel.: 0034 988 347 000. Fax: 0034 988 347 001. E-mail: xmejuto@uvigo.es.
[†] Department of Physical Chemistry, Faculty of Sciences. E-mail: juanferreiro@uvigo.es; gastray@uvigo.es.
[‡] Department of Informatics, ESEI. E-mail: kaderno@gulo.org; galvez@uvigo.es.

10.1021/je1001973
Published on Web 05/19/2010

Table 1. Factor Design Levels: Temperature (*T*), Pressure (*P*), Volume Hydrogen (*H*), Comonomer Ethene Ratio (CER), and Activator Support Ratio (ASR) and Responses for the Experiments: Activity (*A*), Homopolymer (H), Copolymer (C), Overall 1-Octene Content in the Copolymer (OCC), Average Number of Crystallization Temperatures from the Homopolymer (H_c), Copolymer (C_c), Molecular Weight (M_w), and Polydispersity Index (PDI)

factor design level[a]						responses							
experiment no.[b]	*T*/ C	*P*/MPa	*H*/mL	CER	ASR	*A*/(kg of PE)·(mol of cat·h)$^{-1}$	H/%[c]	C/%[c]	OCC/%[d]	H_c/Tn[e]	C_c/Tn[e]	M_w/g·mol^{-1}[f]	PDI[f]
1[g]	313.16	0.6897	0	0.07	15	2.107	100	0	0.41	80.03		354,900	2.95
2	343.16	0.6897	0	0.07	5.335	8.448	100	0	1	76.11		114,000	2.66
3	313.16	1.3793	0	0.07	5.335	6.713	100	0	0.29	80.94		373,200	3.77
4	343.16	1.3793	0	0.07	15	10.880	100	0	0.87	77.06		213,800	2.17
5	313.16	0.6897	50	0.07	5.335	392	67.8	32.2	2.21	76.27	51.26	26,000	2.32
6	343.16	0.6897	50	0.07	15	1.589	87.2	12.8	2.11	72.26	47.36	33,600	1.79
7	313.16	1.3793	50	0.07	15	2.381	75.8	24.2	1.58	79.25	50.46	41,800	4.73
8	343.16	1.3793	50	0.07	5.335	5.040	100	0	0.93	75.8		49,300	2.55
9	313.16	0.6897	0	0.21	5.335	15.387	19.5	80.5	5.71	75.56	75.74	153,200	2.48
10	343.16	0.6897	0	0.21	15	5.440	10.5	89.5	3.98	74.67	55.02	57,500	2
11	313.16	1.3793	0	0.21	15	10.880	52	48	3.02	78.15	48.78	427,600	2.25
12	343.16	1.3793	0	0.21	5.335	26.560	16.1	83.9	3.5	70.97	58.73	463,800	2.53
13	313.16	0.6897	50	0.21	15	1.387	7.5	92.5	7.06	74.47	37.95	32,400	2.15
14	343.16	0.6897	50	0.21	5.335	3	4.9	95.1	5.89	72.43	44.2	47,000	1.94
15	313.16	1.3793	50	0.21	5.335	6.320	55.9	44.1	2.78	78.91	46.57	46,600	3.53
16[g]	343.16	1.3793	50	0.21	15	5.520	14.2	85.8	3.93	75.37	54.71	64,100	2.02
17	328.16	1.0345	25	0.14	10.1675	5.216	62.3	37.7	1.91	77.18	58.88	67,100	2.78
18[g]	328.16	1.0345	25	0.14	10.1675	5.824	72.2	27.8	1.59	77.3	59.56	64,300	2.77
19	328.16	1.0345	25	0.14	10.1675	3.740	66.8	33.2	1.79	77.05	59.01	76,500	2.69
20	298.16	1.0345	25	0.14	10.1675	1.296	74.1	26	1.29	81.01	55.12	13,800	3.04
21	358.16	1.0345	25	0.14	10.1675	26.560	100	0	2.3	67.29		104,500	2.69
22	328.16	0.3448	25	0.14	10.1675	427	11.1	88.9	3.88	75.8	55.43	32,700	2.1
23	328.16	1.3793	25	0.14	10.1675	6.640	66.8	33.3	1.86	77.52	57.07	88,000	2.6
24	328.16	1.0345	0	0.14	10.1675	15.160	62.2	37.8	1.74	75.95	63.82	280,900	2.99
25	328.16	1.0345	75	0.14	10.1675	1.156	42.3	57.7	2.8	74.31	57.41	105,100	3.85
26	328.16	1.0345	25	0	10.1675	4.267	100	0	0.36	79.9		63,500	6.11
27	328.16	1.0345	25	0.28	10.1675	13.200	7	93	6.64	76.27	40.72	95,000	2.05
28	328.16	1.0345	25	0.14	0.5025	42.480	34.7	65.3	2.35	78.36	61.73	204,300	6.93
29	328.16	1.0345	25	0.14	19.8325	1.680	78.8	21.2	1.15	79.24	60.54	63,100	2.48
30	328.16	1.0345	25	0.14	10.1675	4.640	56.2	43.8	1.77	78.63	61.39	95,800	2.72
31[g]	328.16	1.0345	25	0.14	10.1675	5.200	78.4	21.6	1.23	78.75	60.27	71,800	3.08
32	328.16	1.0345	25	0.14	10.1675		83.3	16.7	1.38	77.6	54.71	55,800	2.61

[a] As determined by 2^{v_v-1} factorial design. [b] Experiments were carried out with the Me_2Si(2-Me-4,5 BenzInd)$_2ZrCl_2$ catalyst, silica-supported MAO, the TEA activator, ethene monomer, and oct-1-ene comonomer. Runs shown here were carried out in a randomized fashion. C indicates a center-point replicate. [c] Estimated from the areas in the CRYSTAF profiles determined to be the homopolymer and copolymer. [d] Estimated from the CRYSTAF profile with a calibration curve relating the 1-octene content and Tc. [e] Average number of crystallization temperatures from the homopolymer and copolymer regions in the CRYSTAF profiles. [f] As determined by gas particle chromatography (GPC) with narrow polystyrene standards and the universal calibration curve. [g] Indicates the cases that have been reserved for the validation of the implemented ANNs.

Nv neuron, binary neuron, or McCulloch-Pitts neuron, is an abstraction of biological neurons and the basic unit in an ANN. The artificial neuron receives one or more inputs (representing the one or more dendrites) and sums them to produce an output (synapse). Usually the sums of each node are weighted, and the sum is passed through a nonlinear function known as an activation or transfer function. The canonical form of transfer functions is the sigmoid, but they may also take the form of other nonlinear functions, piecewise linear functions, or step functions. Generally, transfer functions are monotonically increasing. Unlike the simulation modeling, these systems require prior knowledge of the relationship between parameters. The advantage of ANNs consists of their ability to learn from real cases and relearn when new data are input into the system. They are particularly useful in managing different aspects of engineering and science.[16−26] In chemistry, they can be used to solve different types of problems: the classification of objects, the modeling of functional relationships, the storage and retrieval of information, and the representation of large amounts of data.[27,28] This potential suggests many possibilities for the processing of chemical data, and already applications cover a wide area.[29−38]

Materials and Methods

Data Set. Parameters used in the ANNs are shown in Table 1. All experiments were carried out with the Me_2Si(2-Me-4,5 BenzInd)$_2ZrCl_2$ catalyst, silica-supported monoamine oxidase (MAO), tetraethylammonium (TEA) activator, ethene monomer, and 1-octene comonomer. Runs shown here were carried out in a randomized fashion. C indicates a center-point replicate.

Hardware. The equipment used was an Intel Core 2 Quad with 4 GB of RAM, using Xen virtual machines to achieve higher simulation performance.

Software. For the implementation of ANNs was used EasyNN plus V. 12.0, which is a commercial software package provided by Neural Planner Software Ltd. All of the component parts are implemented as C++ reusable classes to simplify future development.

The functioning of the neural network could be described as follows: each neuron from the primary layer collects the data of the input variables and presents them according to an input vector

$$x^p = (x_1^p, x_2^p, ..., x_N^p)^T \quad (1)$$

This input vector spreads toward the intermediate layer by means of the following propagation rule

$$s_i^p = \sum_{j=1}^{N} w_{ji} x_j^p + b_i \quad (2)$$

where N is the number of the network input neurons, w_{ji} is the weight value of the connection between the neuron j from the

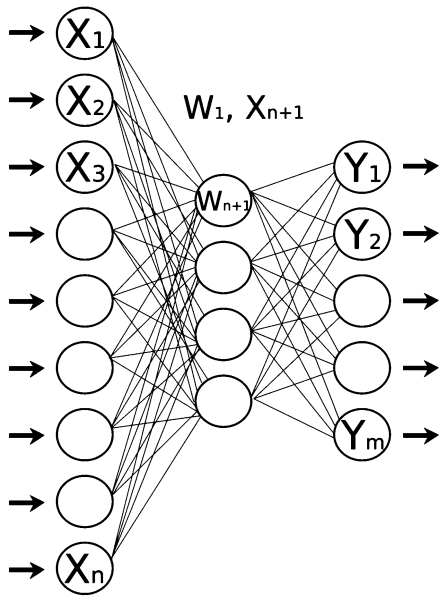

Figure 1. Diagram of perceptron network constituted by a *n*-neuron input layer, a hidden four-neuron layer, and a *m*-output neuron. *W* represents the weight among the various neurons from each layer. X_n are the data of the input variables, and Y_m represent the output data.

Table 2. Adjustments for the Predicted Values of Temperature (*T*), Pressure (*P*), Volume Hydrogen (*H*), Comonomer Ethene Ratio (CER), and Activator Support Ratio (ASR) after the Training of Different ANN Architectures (Coefficient of Determination *R*)

architecture	*T*	*P*	*H*	CER	ASR
7-[3−2]$_2$-5	0.2823	0.6593	0.5248	0.6974	0.3639
7-[3]$_1$-5	0.8665	0.5455	0.8449	0.7935	0.3265
7-[4]$_1$-5	0.7854	0.7386	0.8148	0.7908	0.599
7-[11−6]$_2$-5	0.9988	0.9999	0.9971	0.9992	0.9975
7-[15]$_1$-5	0.9987	0.9914	0.9975	0.9947	0.9511

input layer and the neuron *i* from the intermediate layer, and b_i is the value of the "bias" associated to the neuron *i*. If it is assumed that the activation state of the neuron *i* is the function of the network input vector, then the network output derives from:

$$y_i^p = F_i(s_i^p) \tag{3}$$

Similarly, for any neuron *k* from the output layer, the equations that determine its activation state are:

$$s_k^p = \sum_{i=1}^{L} w_{ik} y_i^p + b_k \tag{4}$$

$$y_k^p = F_k(s_k^p) \tag{5}$$

where *L* is the neuron number of the intermediate layer, w_{ik} is the weight value of the connection between the neuron *i* from the intermediate layer and the neuron *k* from the output layer, and b_k is the value of the "bias" associated with the neuron *k*. The term of error for the output neuron is calculated by means of the following equation

$$E^p = \frac{1}{2}\sum_{k=1}^{M} (d_k^p - y_k^p)^2 \tag{6}$$

and if it adjusts to the previously established value, the training of the neural network finishes here. On the contrary, if it does not adjust to the previously established margins of error, the process would be repeated until reaching the desired error value. The activation equation used in this article is the sigmoid or logistic.

$$F_k(s_k^p) = \frac{1}{1 + e^{-s_k^p}} \tag{7}$$

A back-propagation rule (BP), which is a typical gradient-based learning algorithm, was used as the learning rule in the present work.

$$\Delta_p w_{ik} = -\eta \frac{\partial E^p}{\partial w_{ik}} = \eta (d_k^p - y_k^p) F_k'(s_k^p) y_i^p = \eta \delta_k^p y_i^p \tag{8}$$

This learning rule presents an important limitation, which is the large number of input cases for the training process, but for our study, a large amount of cases were available. This application could be interpreted as an ANN constituted by a primary neural layer (where the data of the input variables would be collected), an output neural layer (where the collected value would be obtained), and one or various intermediate layers (where the convergence work of the neural network would be facilitated) (see Figure 1).

The architecture of ANN is denoted as the following code:

$$N_{\text{in}} - [N_{\text{h1}} - N_{\text{h2}} - N_{\text{h3}}]_e - N_{\text{out}} \tag{9}$$

where N_{in} and N_{out} are the number of neurons in the input layer and output layer, respectively, N_{h1}, N_{h2}, and N_{h3} are the number of neurons in the first, second, and third intermediate layers, respectively, and *e* is the number of hidden layers.

Results and Discussion

Modelization. Different ANN architectures have been studied to find the best neural modelization, which determined the best conditions of ethene + oct-1-ene copolymerization.

The number of neurons in the first layer was seven: activity, homopolymer, copolymer, overall oct-1-ene content in the copolymer, homopolymer Tn, M_w, and polydispersity index. The number of neurons in the intermediate layer was tested between $n/2 + 1$ and $2n + 1$, while the number of intermediate layers was tested between 1 and 3. The number of neurons in the final layers was five (temperature, pressure, hydrogen, comonomer ethene ratio, and activator support ratio).

Table 3. Adjustments for the Predicted Values of Temperature (*T*), Pressure (*P*), Volume Hydrogen (*H*), Comonomer Ethene Ratio (CER), and Activator Support Ratio (ASR) after Validation of Different ANN Architectures (Coefficient of Determination *R*)

architecture	*T*	*P*	*H*	CER	ASR
7-[3−2]$_2$-5	0.5633	0.9392	0.6643	0.6888	0.7701
7-[3]$_1$-5	0.7188	0.4938	0.9379	0.7521	0.7854
7-[4]$_1$-5	0.231	0.2872	0.5639	0.7657	0.7209
7-[11−6]$_2$-5	0.0476	0.8165	0.1023	0.9884	0.9102
7-[15]$_1$-5	0.0934	0.8056	0.1971	0.8841	0.0263

Table 4. Adjustments for the Predicted Values of Temperature (*T*), Pressure (*P*), Volume Hydrogen (*H*), Comonomer Ethene Ratio (CER), and Activator Support Ratio (ASR) for Training and Validation Phase for the Best Architecture 7-[15]$_1$-1 (Coefficient of Determination *R*)

	T/K	*P*/MPa	*H*/mL	CER	ASR
			Training		
R	1	0.9824	0.9991	0.9988	0.9962
RMSE	0.1077	0.0749	1.3320	0.0038	0.6591
			Validation		
R	0.9951	0.9970	0.9995	0.8557	0.9937
RMSE	5.3646	0.0531	1.2175	0.0344	0.6458

Table 5. Experimental Values (Denoted by R Subscript) versus Predicted Values (Denoted by P Subscript) of Temperature (*T*), Pressure (*P*), Volume Hydrogen (*H*), Comonomer Ethene Ratio (CER), and Activator Support Ratio (ASR) Calculated by ANNs for Training and Validation Data

training phase						validation phase		
T_R/K	T_P/K	RMSE	T_R/K	T_P/K	RMSE	T_R/K	T_P/K	RMSE
343.16	343.14	0.02	328.16	327.89	0.27	313.16	321.63	8.47
313.16	313.16	0.00	328.16	328.56	0.40	343.16	336.61	6.55
343.16	343.17	0.01	298.16	298.36	0.20	328.16	328.77	0.61
313.16	313.16	0.00	358.16	358.07	0.09	328.16	327.84	0.32
343.16	343.16	0.00	328.16	328.17	0.01			
313.16	313.16	0.00	328.16	327.97	0.19			
343.16	343.17	0.01	328.16	328.17	0.01			
313.16	313.16	0.00	328.16	328.17	0.01			
343.16	343.16	0.00	328.16	328.17	0.01			
313.16	313.16	0.00	328.16	328.16	0.00			
343.16	343.16	0.00	328.16	328.16	0.00			
313.16	313.16	0.00	328.16	328.14	0.02			
343.16	343.16	0.00	328.16	328.24	0.08			
313.16	313.17	0.01	328.16	328.16	0.00			
P_R/MPa	P_P/MPa	RMSE	P_R/MPa	P_P/MPa	RMSE	P_R/MPa	P_P/MPa	RMSE
0.6897	0.8943	0.2046	1.0345	1.0988	0.0643	0.6897	0.7906	0.1009
1.3793	1.3696	0.0097	1.0345	1.1510	0.1166	1.3793	1.3749	0.0044
1.3793	1.3773	0.0020	1.0345	1.0892	0.0547	1.0345	1.0658	0.0313
0.6897	0.7513	0.0617	1.0345	1.0925	0.0580	1.0345	1.0435	0.0090
0.6897	0.8444	0.1548	0.3448	0.3455	0.0007			
1.3793	1.3715	0.0078	1.3793	1.3261	0.0532			
1.3793	1.3777	0.0016	1.0345	1.0647	0.0302			
0.6897	0.8029	0.1132	1.0345	1.0862	0.0517			
0.6897	0.8686	0.1790	1.0345	1.0526	0.0181			
1.3793	1.3790	0.0003	1.0345	1.0479	0.0134			
1.3793	1.3785	0.0008	1.0345	1.0530	0.0186			
0.6897	0.7660	0.0763	1.0345	1.0449	0.0104			
0.6897	0.7617	0.0721	1.0345	1.0433	0.0088			
1.3793	1.3793	0.0000	1.0345	1.0368	0.0023			
H_R/mL	H_P/mL	RMSE	H_R/mL	H_P/mL	RMSE	H_R/mL	H_P/mL	RMSE
0	0.57	0.57	25	26.44	1.44	0	0	0
0	0	0	25	25.78	0.78	50	52.04	2.04
0	0.03	0.03	25	25.67	0.67	25	26.31	1.31
50	53.74	3.74	25	25.40	0.40	25	24.85	0.15
50	51.93	1.93	25	25.56	0.56			
50	52.70	2.70	25	25.10	0.10			
50	53.46	3.46	0	0	0.00			
0	0.37	0.37	75	74.72	0.28			
0	0.88	0.88	25	25.16	0.16			
0	0	0	25	25.21	0.21			
0	0	0	25	25.10	0.10			
50	51.50	1.50	25	25.17	0.17			
50	51.32	1.32	25	25.13	0.13			
50	51.92	1.92	25	25.06	0.06			
CER_R	CER_P	RMSE	CER_R	CER_P	RMSE	CER_R	CER_P	RMSE
0.07	0.07	0	0.14	0.14	0	0.07	0.14	0.07
0.07	0.08	0.01	0.14	0.14	0	0.21	0.21	0
0.07	0.07	0	0.14	0.14	0	0.14	0.14	0
0.07	0.07	0	0.14	0.14	0	0.14	0.15	0.01
0.07	0.07	0	0.14	0.14	0			
0.07	0.08	0.01	0.14	0.14	0			
0.07	0.07	0	0.14	0.14	0			
0.21	0.22	0.01	0.14	0.14	0			
0.21	0.22	0.01	0	0	0			
0.21	0.21	0	0.28	0.28	0			
0.21	0.21	0	0.14	0.14	0			
0.21	0.22	0.01	0.14	0.14	0			
0.21	0.21	0	0.14	0.14	0			
0.21	0.21	0	0.14	0.14	0			
ASR_R	ASR_P	RMSE	ASR_R	ASR_P	RMSE	ASR_R	ASR_P	RMSE
5.34	4.24	1.10	10.17	9.58	0.59	15.00	13.88	1.12
5.34	4.48	0.86	10.17	9.77	0.40	15.00	14.59	0.41
15	13.96	1.04	10.17	9.74	0.43	10.17	9.66	0.51
5.34	4.66	0.68	10.17	9.75	0.42	10.17	10.17	0
15	13.91	1.09	10.17	9.83	0.34			
15	14.15	0.85	10.17	9.94	0.23			
5.34	4.29	1.05	10.17	9.98	0.19			
5.34	4.21	1.13	10.17	10.00	0.17			
15	14.10	0.90	10.17	10.02	0.15			
15	14.13	0.87	10.17	10.05	0.12			
5.34	4.66	0.68	0.5	0.59	0.09			
15	14.31	0.69	19.83	19.61	0.22			
5.34	4.55	0.79	10.17	10.13	0.04			
5.34	4.93	0.41	10.17	10.16	0.01			

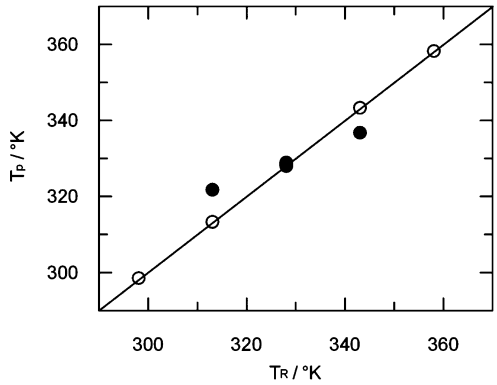

Figure 2. Experimental values of temperature (T_R) versus predicted values (T_P) for ○, training data; and ●, validation data; calculated by ANN 7-[15]$_1$-1.

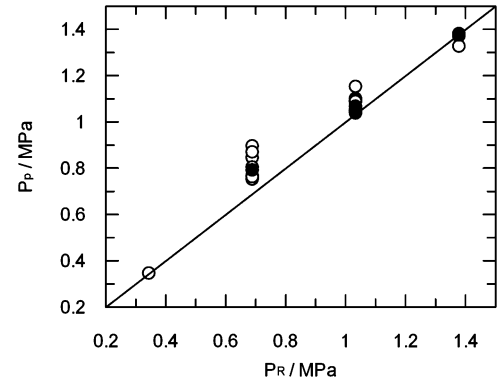

Figure 3. Experimental values of pressure (P_R) versus predicted values (P_P) for ○, training data; and ●, validation data; calculated by ANN 7-[15]$_1$-1.

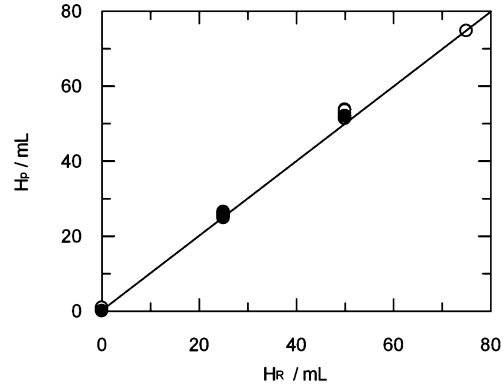

Figure 4. Experimental values of volume of hydrogen (H_R) versus predicted values (H_P) for ○, training data; and ●, validation data; calculated by ANN 7-[15]$_1$-1.

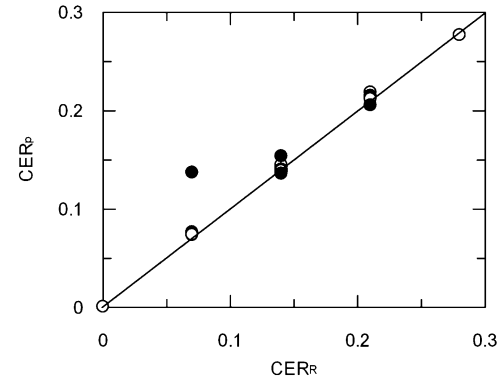

Figure 5. Experimental values of comonomer/ethene ratio (CER_R) versus predicted values (CER_P) for ○, training data; and ●, validation data; calculated by ANN 7-[15]$_1$-1.

For the training of the various ANNs 28 experimental data points calculated by Shan et al.[38,39] were used. The other four cases, not used in the training stage, were reserved for the validations of the ANNs. Table 2 shows the regression adjustments (R) for some of the various architectures studied.

Once the different ANNs were trained, we proceeded to the study of their functioning by using the four cases previously reserved. Table 3 represents the regression adjustments (R) for some of the various architectures studied.

Taking into account the training results for each implemented ANN and the R values for validating cases, we had found a nonsatisfactory fit. This fact is due to the large number of output variables. To solve this problem, we decide to implement five new ANNs with seven neurons in the first layer; activity, homopolymer, copolymer, overall oct-1-ene content in the copolymer, homopolymer, M_w, and polydispersity index. The number of neurons in the intermediate layer was tested between $n/2 + 1$ and $2n + 1$, while the number of intermediate layers was tested between 1 and 3. The number of neurons in the final layer was one for each ANN; temperature, pressure, hydrogen, comonomer ethene ratio, and activator support ratio.

Once the different ANNs were trained, we proceeded to the study of their functioning by using the 4 cases previously reserved.

Selected Architecture. Taking into account the regression adjustment values (R), it has been decided that the most favorable architectures for the prediction of suitable conditions of temperature, ethene pressure, hydrogen amount, comonomer ethene ratio, and activator support ratio used that determine the copolymerization are the typologies 7-[15]$_1$-1. Table 4 shows R values for training and validation set for the different ANNs. Table 5 shows experimental values (denoted by R subscript) versus predicted values (denoted by P subscript) of temperature (T), pressure (P), volume hydrogen (H), comonomer ethene ratio (CER), and activator support ratio (ASR) calculated by ANNs for training and validation data.

As shown in Figures 2 to 6, the linear adjustments of the training values are very satisfactory. The high R values demonstrate the good correlation existing between experimental values and predicted values by the ANN for training. To know the error committed by the ANN for each of the output variables, it has been calculated or quantified in terms of root-mean-square error (RMSE) for the three variables. Values obtained were 0.1077, 0.0749, 1.3320, 0.0038, and 0.6591, respectively, which denotes the proper training of the ANN in question.

As mentioned before, the four reserved cases were used to verify the functioning of the ANN after carrying out its proper training. R values obtained for each of the output variables were 0.9951, 0.9970, 0.9995, 0.8557, and 0.9937, respectively (Figure 2 to 6). The RMSE for the five output variables were also calculated, presenting the values of 5.3646, 0.0531, 1.2175, 0.0344, and 0.6458, respectively, which denotes the proper training of the ANN in question. The importance of the variables selected for the ANN has been determined. This value is the sum of the weights of the input neurons to all intermediate neurons (Table 6).

Conclusions

Results obtained show a high coefficient of linear regression between the values predicted by the ANN for the training cases in comparison with the real values of temperature, pressure, the amount of hydrogen, comonomer ethene ratio, and activator support ratio (Table 4). The accuracy of the neural network developed was tested with four cases of data, which was not taken into account to establish the aforementioned models.

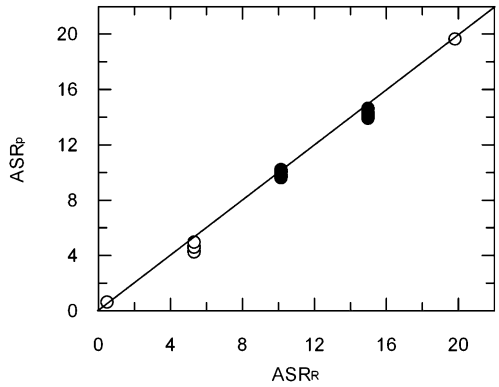

Figure 6. Experimental values of activator/support ratio (ASR_R) versus predicted values (ASR_P) for ○, training data; and ●, validation data; calculated by ANN 7-$[15]_1$-1.

Table 6. Importance of Variables Considered for the Best Typologies (7-$[15]_1$-1) for Input Variables of Temperature (*T*), Pressure (*P*), Volume Hydrogen (*H*), Comonomer Ethene Ratio (CER), and Activator Support Ratio (ASR)

	output variables				
input variables	*T*	*P*	*H*	CER	ASR
homopolymer/Tn	41.30	129.96	81.94	55.49	67.54
overall oct-1-ene content in the copolymer/%	41.06	131.98	72.23	32.57	66.64
M_w/g·mol^{-1}	40.22	123.98	72.57	17.90	71.52
homopolymer/%	35.33	85.92	65.78	31.67	50.52
polydispersity index	31.20	142.04	65.32	37.83	102.45
copolymer/%	29.79	63.63	47.08	32.84	60.86
activity/(kg of PE)·(mol of cat·h)$^{-1}$	10.48	68.14	28.59	22.49	26.67

Neural networks provided us a good tool to predict ideal conditions of copolymerization and thus could help the automation of appropriate conditions for the copolymerization. Furthermore, the ANN implemented here should be optimized according to known copolymerization new parameters to extend its use to another type of copolymerization.

Literature Cited

(1) Hamielec, A. E.; Soares, J. B. P. Polymerization reaction engineering-Metallocene catalysts. *Prog. Polym. Sci.* **1996**, *21*, 651–706.
(2) Gupta, V. K.; Satish, S.; Bhardwaj, I. Metallocene complexes of group 4 elements in the polymerization of monoolefins. *Rev. Macromol. Chem. Phys.* **1994**, *3*, 439–514.
(3) Huang, J.; Rempel, G. L. Ziegler-Natta catalysts for olefin polymerization: Mechanistic insights from metallocene systems. *Prog. Polym. Sci.* **1995**, *20*, 459–526.
(4) Reddy, S. S.; Sivaram, S. Homogeneous metallocene-methylaluminoxane catalyst systems for ethylene polymerization. *Prog. Polym. Sci.* **1995**, *20*, 309–367.
(5) Soares, J. B. P.; Hamielec, A. E. General dynamic mathematical modelling of heterogeneous Ziegler-Natta and metallocene catalyzed copolymerization with multiple site types and mass and heat transfer resistances. *Polym. React. Eng.* **1995**, *3*, 261–324.
(6) Elias, H. G. *Ulmann's Encyclopedia of Industrial Chemistry*; VCH Publishers: New York, 1992.
(7) Whiteley, K. S.; Heggs, T. G.; Koch, H.; Mawer, R. L.; Immel, W. *Ulmann's Encyclopedia of Industrial Chemistry*; VCH Publishers: Weinheim, 1992.
(8) Bishop, M. C. *Neural Networks for Pattern Recognition*; Oxford University Press: New York, 1995.
(9) Rosenblatt, F. The perceptron: a probabilistic model for information storage and organization in the brain. *Psych. Rev.* **1958**, *65*, 386–408.
(10) Xu, K.; Xie, M.; Tang, L.; Ho, S. L. Application of neural networks in forecasting engine system reliability. *Appl. Soft. Comput.* **2003**, *2*, 255–268.
(11) McCulloch, W.; Pitts, W. A logical calculus of the ideas immanent in nervous activity. *Bull. Math. Biophys.* **1943**, *7*, 115–133.
(12) Castillo, E.; Gutiérrez, J. M.; Hadi, A. S.; Lacruz, B. Some applications of functional networks in statistics and engineering. *Technomet.* **2001**, *43*, 10–24.
(13) Grinn-Gofron, A.; Strzelczak, A. Artificial neural network models of relationships between *Cladosporium* spores and meteorological factors in Szczecin (Poland). *Granja* **2008**, *47*, 305–315.
(14) Rodríguez-Rajo, F. J.; Astray, G.; Ferreiro-Lage, J. A.; Aira, M. J.; Jato-Rodriguez, V.; Mejuto, J. C. Evaluation of atmospheric *Poaceae* pollen concentration using a neural network applied to a coastal Atlantic climate region. *Neural Networks* **2010**, *23*, 419–425.
(15) Rumelhart, D. E.; McClelland, J. L. *Parallel distributed processing: Exploration in the microstructure of cognition*; MIT Press: Cambridge, MA, 1986.
(16) Ni, H.; Gunasekaran, S. Food quality prediction with neural networks. *Food. Technol.* **1998**, *52*, 60–65.
(17) Xie, G.; Xiong, R. Use of hyperbolic and neural network models in modeling quality changes of dry peas in long time cooking. *J. Food Eng.* **1999**, *41*, 151–162.
(18) Park, B.; Chen, Y. R.; Whittaker, A. D.; Miller, R. K.; Hale, D. S. Neural network modeling for beef sensory evaluation. *Trans. ASAE* **1994**, *37*, 1547–1553.
(19) Latrille, E.; Corrieu, G.; Thibault, J. pH prediction and final fermentation time determination in lactic acid batch fermentations. *Comput. Chem. Eng.* **1993**, *17*, 423–428.
(20) Dornier, M.; Decloux, M.; Trystram, G.; Lebert, A. Dynamic modeling of crossflow microfiltration using neural networks. *J. Membr. Sci.* **1995**, *98*, 263–273.
(21) Erenturk, S.; Erenturk, K. Comparison of genetic algorithm and neural network approaches for the drying process of carrot. *J. Food Eng.* **2007**, *78*, 905–912.
(22) Movagharnejad, K.; Nikzad, M. Modeling of tomato drying using artificial neural network. *Comp. Elect. Agric.* **2007**, *59*, 78–85.
(23) Martynenko, A. I.; Yang, S. X. Biologically inspired neural computation for ginseng drying rate. *Biol. Eng.* **2006**, *95* (3), 385–396.
(24) González-Sáiz, J. M.; Garrido-Vidal, D.; Pizarro, C. Modelling the industrial production of vinegar in aerated-stirred fermentors in terms of process variables. *J. Food Eng.* **2009**, *91*, 183–196.
(25) Astray, G.; Castillo, X.; Ferreiro-Lage, J. A.; Gálvez, J. F.; Mejuto, J. C. Artificial neural networks: a promising tool to evaluate the authenticity of wine. *J. Food* **2010**, *8*, 79–86.
(26) Gasteiger, J.; Zupan, J. Neural Networks in Chemistry. *Angew. Chem., Int. Ed.* **1993**, *32*, 503–527.
(27) Zupan, J.; Gasteiger, J. Neural networks: A new method for solving chemical problems or just a passing phase. *Anal. Chim. Acta* **1991**, *248*, 1–30.
(28) Kvasnicka, V.; Sklenak, S.; Pospichal, J. Application of recurrent neural networks in chemistry. Prediction and classification of ^{13}C NMR chemical shifts in a series of monosubstituted benzenes. *J. Chem. Inf. Comput. Sci.* **1992**, *32*, 742–747.
(29) Kvasnicka, V. An application of neural networks in chemistry. Prediction of ^{13}C NMR chemical shifts. *J. Math. Chem.* **1991**, *6*, 63–76.
(30) Jalali-Heravi, M. Neural networks in analytical chemistry. *Methods Mol. Biol. (Totowa, NJ, U.S.)* **2008**, *458*, 81–121.
(31) Lazzús, J. A. Neural Network Based on Quantum Chemistry for Predicting Melting Point of Organic Compounds. *Chin. J. Chem. Phys.* **2009**; doi:10.1088/1674-0068/22/01/19-26.
(32) Zou, Y.; Johnson, M.; Tsai, C. C. Modeling aromatic nitration reactions using graph-theoretic transforms. *J. Chem. Inf. Comput. Sci.* **1990**, *30*, 442–450.
(33) Kvasnicka, V.; Pospichal, J. Application of neural networks in chemistry. Prediction of product distribution of nitration in a series of monosubstituted benzenes. *J. Mol. Struct.* **1990**, *235*, 227–242.
(34) Elrod, D.; Maggiora, G. M.; Trenary, R. G. Applications of Neural Networks in Chemistry, Prediction of Electrophilic Aromatic Substitution Reactions. *J. Chem. Inf. Comput. Sci.* **1990**, *30*, 477–484.
(35) Elrod, D. W.; Maggiora, G. M.; Trenary, R. G. Application of Neural Networks in Chemistry. 2. A General Connectivity Representation for the Prediction of Regiochemistry. *Tetrahedron Comput. Methodol.* **1990**, *3*, 163–174.
(36) Molga, E. J.; van Worzik, B. B. A.; Westerterp, K. R. Neural networks for modelling of chemical reaction systems with complex kinetics: oxidation of 2-octanol with nitric acid. *Chem. Eng. Process.* **2000**, *39*, 323–334.
(37) Ramirez-Beltran, N. D.; Jackson, H. Application of neural networks to chemical process control. *Comput. Ind. Eng.* **1999**, *37*, 387–390.
(38) Shan, C. L. P.; Soares, J. B. P.; Penlidis, A. Ethylene/1-octene copolymerization studies with in situ supported metallocene catalysts: Effect of polymerization parameters on the catalyst activity and polymer microstructure. *J. Polym. Sci., Part A: Polym. Chem.* **2002**, *40*, 4426–4451.
(39) Chauvin, Y.; Rumelhart, D. E. *Backpropagation: Theory architectures and applications*; Mawah, Lawrence Erlbaum Associates: NJ, 1995.

Received for review March 1, 2010. Accepted May 7, 2010. G.A. thanks the "Xunta de Galicia" for a training research grant (P.P. 0000 300S 14008).

JE1001973